A POSSIBLE EXPLANATION FOR THE ASSOCIATION BETWEEN OBESITY AND CANCER RISK

by
Yifan Zhang

A thesis submitted to Johns Hopkins University in conformity with the requirements for the degree of Master of Science

Baltimore, Maryland

April 2020

Abstract

Obesity is known to be associated with increased risk in various cancer types. Several biological mechanisms underlying this association have been proposed, including alterations in sex hormone metabolism, insulin and insulin-like growth factor signaling, and adipokines and the inflammatory system, but there are limitations to all these previously proposed mechanisms. We explore a new explanation for the association, that is, individuals with higher BMIs have larger organs, which consist of more cells that are at risk of becoming cancerous. We search through literature to find studies on the association between BMI or body weight and organ size. We find that for cancers originating in the gallbladder, thyroid, liver, kidney, pancreas, and gastric cardia, the estimated relative increases in organ sizes due to obesity are comparable to the relative increases in risk of cancer due to obesity reported by the International Agency for Research on Cancer (IARC) Handbook Working Group.

Thesis Advisor: Cristian Tomasetti

Thesis Reader: Bahman Afsari

Acknowledgements

I would like to thank my advisor, Cristian Tomasetti, who has always provided invaluable guidance. I would also like to thank Bahman Afsari for his valuable feedback on my work. I am also truly grateful to all the faculty and friends I've met for helping me learn and grow during my time in the department. Last, I would like to thank my family for all their love and support.

Table of Contents

List of Tables

List of Figures

1. Introduction

1.1 Obesity

Overweight and obesity are conditions characterized by excess body fat. The body mass index (BMI) is commonly used to screen for overweight or obesity. Though not a direct measurement of body fat, BMI has been shown to be moderately correlated with more direct measures of body fat obtained from skinfold thickness measurements and dual X-ray absorptiometry (Wohlfahrt-Veje et al. 2014). BMI is calculated as weight in kilograms divided by square of height in meters. A BMI of 18.5-24.9 is considered normal, 25.0-29.9 overweight, and >30.0 obese. Obesity can be further classified into class 1 (BMI 30.0-34.9), class 2 (BMI 35.0-39.9) and class 3 (BMI > 40.0).

Obesity has risen to a major global public health challenge. The worldwide obesity prevalence has nearly tripled since 1975, with around 13% of the world's adult population being obese and 39% being overweight in 2016 (WHO 2020). Despite the noticeable increasing trends, no nation has been successful in reducing its obesity rate in the 33 years from 1980 to 2013 (Ng et al. 2014).

1.2 Obesity and Cancer Risk

Obesity is known to increase risks of diseases including cardiovascular diseases, type 2 diabetes, and certain types of cancer. The International Agency for Research on Cancer (IARC) Handbook Working Group has found sufficient evidence that overweight and obesity lead to significantly increased risk in cancer in 13 organs: esophagus (adenocarcinoma), gastric cardia, colon and rectum, liver, gallbladder, pancreas, breast (postmenopausal), corpus uteri, ovary, kidney (renal cell), meningioma, thyroid and multiple myeloma (Lauby-Secretan et al. 2016).

Several biological mechanisms underlying the association between obesity and increased cancer risk have been proposed, including alterations in sex hormone metabolism, insulin and insulin-like growth factor (IGF) signaling, and adipokines and the inflammatory system (Renehan et al. 2015). However, these hypotheses all have caveats, and the true mechanisms underlying the increased cancer risk have yet to be fully uncovered.

Here, we propose a new possible mechanism: individuals with higher BMIs have larger organs, which consist of more cells that are at risk of becoming cancerous.

2. Methods

We were interested in how organ sizes of individuals with BMIs of 30, 35, 40, 45, and 50 compared to organ sizes of individuals with a lean BMI of 22. To investigate the relationship between BMI and sizes of various organs, we searched through literature. Though studies have been done on individuals with BMIs falling in the overweight and obese range, cases beyond class 1 obesity (BMI 30.0-34.9) have rarely been considered. Thus, we used linear extrapolations to extend the analysis to a full range of BMI values. Steps taken in the analysis of seven cancer sites (gallbladder, thyroid, liver, kidney, pancreas, gastric cardia, and corpus uteri) are further detailed below.

2.1 Gallbladder

Stone et al. studied gallbladder function in healthy, gallstone-free individuals (Stone et al. 1992). Seven subjects with normal BMI (BMI < 25.5) and seven subjects with high BMI (BMI > 33) were recruited. Subjects were given liquid emptying stimuli to produce maximal gallbladder emptying, and their gallbladder volumes were measured every 20 minutes during a 2-hour period. The serial measurements were made by scanning with an ATL Ultrasound System which produced longitudinal and transverse images from which length and diameter measurements at 1-cm intervals were attained and used to calculate volume by the sum-of-cylinders technique. Residual volume was then taken as the minimal gallbladder volume recorded during the 2-hour period.

Subjects in the normal BMI group (22 ± 1) had an average gallbladder residual volume of 4.2 (± 1.3) ml compared to 8.4 (± 2.3) ml in the high BMI group (36 ± 1). Assuming a linear relationship between BMI and gallbladder residual volume, this translates into a 0.3 ml increase per BMI unit.

Since nearly all gallbladder cancers begin in glandular cells that line the inner surface

of the gallbladder, we are interested in comparing the inner surface areas of the organ corresponding to different BMIs. We only had data for the relationship between BMI and gallbladder residual volume though, so we computed gallbladder volumes corresponding to different BMIs and then estimated inner surface areas corresponding to different volumes of the gallbladder. More specifically, literature shows a normal gallbladder measures around 7-10 cm in length and 2-3.5 cm in diameter with a wall thickness of 2-3 mm (Bisset et al. 2008). We took the midpoints of these measurements and approximated the gallbladder as a spheroid, assuming that the relative proportions of the organ measurements stay the same with increases in organ size (Supp. Figure 1).

2.2 Thyroid

Sahin et al. studied sizes of thyroid glands in Turkish Adults (Şahin et al. 2015). The study enrolled 292 females and 169 males, ranging from 18 to 61 years of age, all of whom had normally functioning thyroid glands. The Logiq 5 Pro ultrasound machine was used to scan images of each thyroid lobe. Craniocaudal and sagittal measurements were attained from the longitudinal image, and the transverse measurement was obtained from the transverse image. The ellipsoid formula was then used to estimate the volume of each lobe.

In males, regression of total thyroid volume in mL (y) on weight in kg (x) gave rise to the equation:

$$y = 0.1433x + 2.9141.$$

In females, the linear regression equation was:

$$y = 0.1019x + 5.1557.$$

The range of weights in females was ~45 kg to ~100 kg, and in males ~60 kg to ~ 110 kg. We are interested in the relationship between thyroid size and BMI rather than weight but it is easy to link these two together as BMI is calculated as weight (in kilograms) divided by height (in meters) squared. Height was held constant at the average height in the U.S., which

is 176.0 cm for men and 161.9 cm for women, while weights corresponding to different BMI values were recorded and used to estimate respective thyroid volumes.

2.3 Liver

In a study by Gallagher et al., overweight and obese adults (BMI 25 to <41) with type 2 diabetes were enrolled in a diet and exercise weight-loss intervention program, and changes in various organ sizes (skeletal muscle, heart, liver, kidney, spleen, and pancreas) after the intervention were measured (Gallagher et al. 2017). MRI scans with 5-mm slice thickness were acquired and analyzed to obtain volume estimates, which were then converted to mass estimates by assuming a 1.04 kg/L density for the liver.

At the study baseline, the women weighed on average 82 ± 14 kg, and had an average liver weight of 1.76 ± 0.50 kg; the men weighed on average 93 ± 8 kg, and had an average liver weight of 1.90 ± 0.40 kg. After two years of weight-loss intervention, the subjects weighed on average 5.21 ± 0.74 kg less while MRI-derived measurements showed that their liver weighed 0.11 ± 0.03 kg less. This suggests a 0.02 kg decrease in liver weight per 1 kg decrease in body weight.

Again, to get measurements in terms of BMI, height was held constant at the average U.S. height while weights corresponding to different BMI values were recorded and used to estimate respective liver masses. Since mass is proportional to volume, the ratios of liver masses corresponding to different BMI values are equal to the ratios of liver volumes corresponding to different BMI values.

2.4 Kidney: Renal-cell

The most common type of kidney cancer is renal cell carcinoma, which originates in the lining of the proximal convoluted tubule. No information regarding effects of obesity on the dimensions of the proximal tubule could be found, so instead, here we assume that the surface area of the proximal tubule increases proportionally with kidney volume.

In the same study mentioned above, Gallagher et al. also investigated changes in kidney size as a result of weight loss (Gallagher et al. 2017). At the study baseline, the women weighed on average 82 ± 14 kg, and had an average kidney weight of 0.38 ± 0.11 kg; the men weighed on average 93 ± 8 kg, and had an average kidney weight of 0.46 ± 0.08 kg. After two years of weight-loss intervention, the subjects weighed on average 5.21 ± 0.74 kg less while MRI-derived measurements showed that their kidney weighed 0.02 kg less. This suggests a 0.0038 kg decrease in kidney weight per 1 kg decrease in body weight. The ratios of kidney volumes corresponding to different BMI values were obtained using the same methods as for the liver calculations described above.

2.5 Pancreas

Saisho et al. studied the effect of gender, obesity and type-2 diabetes on pancreas volumes (Saisho et al. 2007). The study enrolled 997 females and 724 males (1721 total) over the age of 20, all of whom had normally functioning pancreata. Whole-body CT scans of subjects were acquired. Fat was differentiated from parenchymal tissue based on the differential density of the two types of cells. Total parenchymal volume of the pancreas was calculated as the sum of volumes from each CT section, which was obtained by multiplying parenchymal area in a CT slice (pixel area in cm^2) by the CT slice thickness. The regression equation relating parenchymal pancreas volume in cm^3 (y) to BMI (x) was given as:

$$y = 34.6 + 0.55x.$$

2.6 Gastric Cardia

The stomach has five main regions, the cardia, the fundus, the body, the antrum, and the pylorus. No studies were found that specifically address the size of the gastric cardia in relation to BMI, so we assumed that the proportions of the regions of the stomach remain fixed. In other words, the size of the cardia increases proportionally with the size of the whole stomach.

Geliebter measured gastric capacity in four lean and four obese subjects (Geliebter 1988). A latex gastric balloon was inserted into the stomach and after each inflation of 100 ml, subjects would rate their discomfort on a scale from 1 (none) to 10 (extreme). Stomach capacity was characterized as the volume of the gastric balloon when the subject reported a discomfort of 10. The mean gastric capacity for lean subjects (mean BMI = 22.3) was 1100 ml, and for obese subjects (mean BMI = 31.5) was 1925 ml. This translates into a 90 ml increase per BMI unit.

Almost all stomach cancers are adenocarcinomas, which develop from cells that line the inside of the stomach. To compute surface area, the stomach is approximated as a spheroid. The average-sized human stomach has a greater curvature that measures at 26-31 cm (Ferrua & Singh 2011). The average volume of the stomach is 0.94 L, and using 28.5 cm as the major axis length (midpoint of the greater curvature reported above), the minor axis length is derived to be approximately 8 cm. These measurements allow us to define the shape of the stomach and thus estimate its surface area given its volume (Supp. Figure 2).

2.7 Corpus Uteri

Parmar et al. studied uterine dimensions in 80 women (40 parous and 40 nulliparous) (Parmar et al. 2016). Study participants excluded those who were pregnant, in menstrual cycle or had a pathological uterus. Measurements of uterine length, width and wall thickness were obtained with high resolution ultrasonography.

The mean uterine length of parous women was 8.63 cm for those with a body weight 51-60 kg, and 9.06 cm for those with a body weight 61-70 kg. In nulliparous women, mean uterine length was 7.08 cm for those with a body weight 51-60 kg, and 7.45 cm for those with a body weight 61-70 kg. This translates into an increase in uterine length of 0.43 cm in parous women, and 0.37 cm in nulliparous women per 10 kg increase in body weight.

According to the U.S. Census Bureau's Current Population Survey in 2018, 49.8 percent of women

aged 15 to 44 had never had children (U.S. Census Bureau 2018). Taking this into account, the weighted increase in uterine length is 0.40 cm per 10 kg increase in weight.

Parmar et al. only reported the correlation between uterine length and body weight but not other dimensions of the uterus. We chose to approximate the corpus part of the uterus as a cone, where the ratio of the length to base diameter of the cavity of body of the uterus was taken to be 1.9 (Umar et al. 2017), and assumed that base diameter increases proportionally with length as body weight increases (Supp. Figure 3). Again, to get measurements in terms of BMI, height was held constant at the average U.S. height while weights corresponding to different BMI values were recorded and used to estimate respective uterus inner surface area.

3. Results

Our estimates of increases in organ size when going from normal weight (BMI=22) to extreme obesity (BMI=50) are provided in Table 1. The gallbladder, liver, and gastric cardia are estimated to more than double in size for extremely obese individuals, while other organs are expected to undergo a smaller increase in size. The estimated relative increases in organ sizes due to obesity are comparable to the relative increases in risk of cancer due to obesity in all cancer types except for corpus uteri.

Table 1: Extrapolated relationship between BMI and organ size, and increase in cancer risk

Cancer type	**Gender**	**Relative Organ Size of BMI Categories Compared to Normal BMI=22**					**Relative Risk of Cancer***
		BMI 30	**BMI 35**	**BMI 40**	**BMI 45**	**BMI 50**	
Gallbladder	Combined	1.35	1.55	1.74	1.91	2.08	1.3 (1.2-1.4)
Thyroid	M	1.28	1.46	1.63	1.81	1.98	1.1 (1.0-1.1)
	F	1.19	1.31	1.44	1.56	1.68	
Liver	M	1.38	1.62	1.86	2.09	2.33	1.8 (1.6-2.1)
	F	1.36	1.58	1.80	2.02	2.24	
Kidney: renal-cell	M	1.26	1.42	1.59	1.75	1.91	1.8 (1.7-1.9)
	F	1.28	1.46	1.63	1.81	1.98	
Pancreas	Combined	1.09	1.15	1.21	1.27	1.33	1.5 (1.2-1.8)
Gastric cardia	Combined	1.41	1.63	1.84	2.04	2.23	1.8 (1.3-2.5)
Corpus uteri	F	1.20	1.33	1.47	1.62	1.77	7.1 (6.3-8.1)

* Relative risk of highest BMI category (BMI ≥ 40.0) evaluated versus normal BMI (18.5-24.9) (Lauby-Secretan et al. 2016).

4. Discussion

Our findings suggest that obesity may induce an increase in the number of cells forming an organ and thus an increase in risk of cancer originating from that organ. This mechanism appears sufficient to explain the increase in cancer risk in the gallbladder, thyroid, liver, kidney, pancreas, and gastric cardia linked to extreme obesity, but not the massive increase in cancer risk in the corpus uteri, suggesting that other factors may be at play in uterine cancer in the obese. To further validate our findings, our analyses could be extended to other organs for which there is sufficient evidence of an increase in cancer risk as a result of excess body fat as reported by IARC.

In analyzing the pancreas, we considered only parenchymal tissue as we were able to find a study that separated parenchymal tissue from fat. We weren't able to find such information for other organs, so our estimates of organ size ratios may be larger than if the estimates were based only on non-fat tissue. However, most estimates should be unaffected since adipose tissue is not commonly found in most organs. Ectopic fat could though accumulate in some organs such as the liver or kidney, but the fat content does not differ greatly between healthy and obese individuals. Specifically, comparing obese to normal weight individuals, the median fat content in the liver is 4.57% vs 1.11%, and in the kidney 1.35% vs 0.64% (Sijens et al. 2010). Thus, the larger liver and kidney volumes measured in obese individuals are a result of an increase in parenchymal and not fat cells.

Our analyses were based on literature search performed to understand how organ dimensions are associated with BMI or body weight. Such studies were scarce and use of information from these studies lead to limitations in our results. Studies often involved subjects with BMIs that did not cover the full range of BMI values we were interested in (BMI 22-50). In the Gallagher study from which data on liver and kidney size were used, subjects had BMI values up to only 41. In the study on stomach size, subjects had BMI

values up to only 35, and in the uterus study, women weighed only up to 70 kg. Thus, our analysis was based on extrapolations in which we were making estimations of organ sizes associated with extreme BMI values that were beyond the original observation range. That is, we were assuming that the trends of increasing organ sizes found in ranges of lower BMI values would extend to ranges of higher BMI values. To validate whether our assumptions are acceptable, we would need data across a full range of BMI.

Other limitations of some studies include small sample size, with the gallbladder study having enrolled 14 subjects and the gastric capacity study having enrolled only 8. In addition, the gastric capacity study measured capacity in intervals of 100 ml, so measurements obtained were not precise, and maximum capacity was based on subject reporting of extreme discomfort, which different individuals may have different tolerance of. Both the gallbladder study and the gastric capacity study were conducted over 20 years ago, so a more recent study enrolling a larger set of individuals and using more advanced measurement technology would be needed to consolidate these findings. However, the gallbladder and stomach, being hollow organs, may undergo changes in size due to oral intake and thus accurate measurements may be hard to obtain, which could explain why data on these two organs were scarce, which led us to using studies that had evident limitations.

The IARC working group reported relative risks for gastric cardia cancer and renal cell cancer, but we could not find information on the size of the cardia or the proximal convoluted tubule in relation to BMI, so increases in size of the entire stomach and kidney were used, and it was assumed that all parts of an organ increase proportionally with increasing BMI.

Most studies we found compared organ sizes between a healthy group and an overweight or obese group, or reported on values of organ sizes across a range of BMI. The Gallagher study, though, compared organ sizes in the same set of subjects, before and after

weight loss. It will be interesting, in the future, to study whether weight loss can lead to shrinking in size of all organs analyzed in this study and thus a decrease in cancer risk.

5. Supplementary

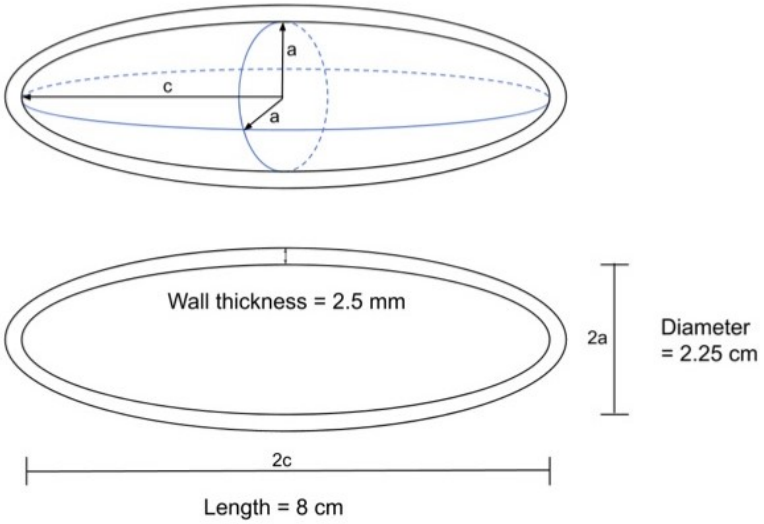

Figure 1: Approximation of gallbladder as spheroid.

Surface area and volume formulas for spheroid:

$$V = \frac{4}{3}\pi a^2 c$$

$$S = 4\pi(\frac{a^{2p} + 2a^p c^p}{3})^{1/p},\ p \approx 1.6075$$

Estimate of gallbladder inner surface area given volume:

$$a = 1.125 \text{ cm},\ c = 4\text{cm}$$

$$c = 3.56a$$

$$V = \frac{4}{3}\pi a^2 (3.56a) = 14.91a^3$$

$$S = 4\pi(\frac{a^{3.2} + 2a^{1.6}(3.56a)^{1.6}}{3})^{1/1.6} = 4\pi(5.42a^{3.2})^{1/1.6} = 36.13a^2$$

$$S = 36.13 \times \left(\frac{V}{14.91}\right)^{2/3}$$

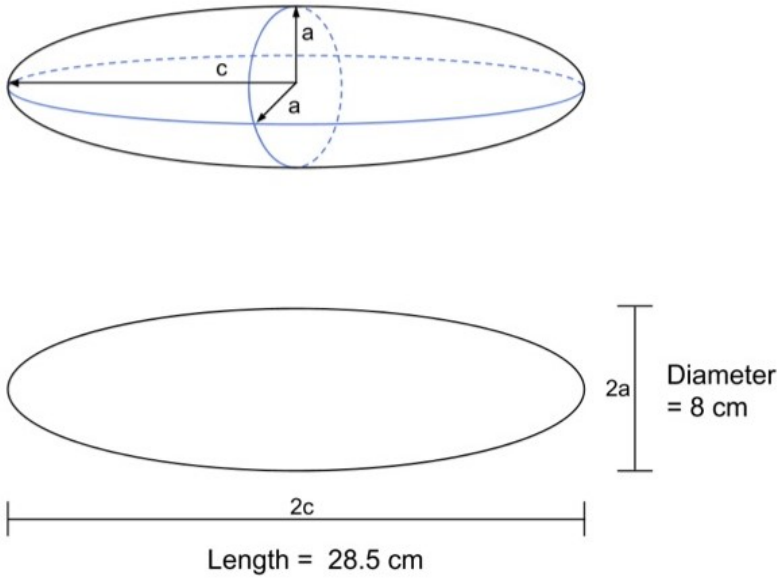

Figure 2: Approximation of stomach as spheroid.

Surface area and volume formulas for spheroid:

$$V = \frac{4}{3}\pi a^2 c$$

$$S = 4\pi(\frac{a^{2p} + 2a^p c^p}{3})^{1/p},\ p \approx 1.6075$$

Estimate of stomach surface area given volume:

$$a = 4 \text{ cm},\ c = 14.25 \text{ cm}$$

$$c = 3.56a$$

$$V = \frac{4}{3}\pi a^2 (3.56a) = 14.91a^3$$

$$S = 4\pi(\frac{a^{3.2} + 2a^{1.6}(3.56a)^{1.6}}{3})^{1/1.6} = 4\pi(5.42a^{3.2})^{1/1.6} = 36.13a^2$$

$$S = 36.13 \times \left(\frac{V}{14.91}\right)^{2/3}$$

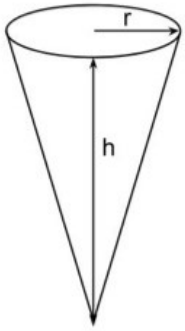

Figure 3: Approximation of uterine cavity as cone.

Surface area formula for cone:

$$S = \pi r\left(r + \sqrt{h^2 + r^2}\right)$$

Estimate of uterus cavity of body surface area given uterine length:

$$r = \frac{h}{3.8}$$

$$S = \pi(\frac{h}{3.8})\left(\frac{h}{3.8} + \sqrt{h^2 + (\frac{h}{3.8})^2}\right) = 1.07h^2$$

6. References

Bisset, R. A. L, et al. *Differential Diagnosis in Abdominal Ultrasound*. Elsevier India, 2008.

Ferrua, Maria J., and R. Paul Singh. "Understanding the Fluid Dynamics of Gastric Digestion Using Computational Modeling." *Procedia Food Science*, vol. 1, 2011, pp. 1465–1472., doi:10.1016/j.profoo.2011.09.217.

Gallagher, Dympna, et al. "Changes in Skeletal Muscle and Organ Size after a Weight-Loss Intervention in Overweight and Obese Type 2 Diabetic Patients." *The American Journal of Clinical Nutrition*, vol. 105, no. 1, 2016, pp. 78–84., doi:10.3945/ajcn.116.139188.

Geliebter, Allan. "Gastric Distension and Gastric Capacity in Relation to Food Intake in Humans." *Physiology & Behavior*, vol. 44, no. 4-5, 1988, pp. 665–668., doi:10.1016/0031-9384(88)90333-2.

Lauby-Secretan, Béatrice, et al. "Body Fatness and Cancer — Viewpoint of the IARC Working Group." *New England Journal of Medicine*, vol. 375, no. 8, 2016, pp. 794–798., doi:10.1056/nejmsr1606602.

Ng, Marie, et al. "Global, regional, and national prevalence of overweight and obesity in children and adults during 1980–2013: a systematic analysis for the Global Burden of Disease Study 2013." *The Lancet*, vol. 384, no. 9945, 2014, pp. 766-781., doi:10.1016/S0140-6736(14)60460-8.

Parmar, Ajay M., et al. "Sonographic Measurements of Uterus and Its Correlation With Different Parameters in Parous and Nulliparous Women." International Journal of Medical Science and Education, vol. 3, no. 3, 2016, pp. 306-310.

Renehan, Andrew G., et al. "Adiposity and Cancer Risk: New Mechanistic Insights from Epidemiology." *Nature Reviews Cancer*, vol. 15, no. 8, 2015, pp. 484–498., doi:10.1038/nrc3967.

Şahin, Ertan, et al. "Regional Reference Values of Thyroid Gland Volume in Turkish Adults." *Srpski Arhiv Za Celokupno Lekarstvo*, vol. 143, no. 3-4, 2015, pp. 141–145., doi:10.2298/sarh1504141s.

Saisho, Yoshifumi, et al. "Pancreas Volumes in Humans from Birth to Age One Hundred Taking into Account Sex, Obesity, and Presence of Type-2 Diabetes." *Clinical Anatomy*, vol. 20, no. 8, 2007, pp. 933–942., doi:10.1002/ca.20543.

Sijens, Paul E, et al. "MRI-Determined Fat Content of Human Liver, Pancreas and Kidney." *World Journal of Gastroenterology*, The WJG Press and Baishideng, 28 Apr. 2010, www.ncbi.nlm.nih.gov/pmc/articles/PMC2860076/.

Stone, Bradford G., et al. "Gallbladder Emptying Stimuli in Obese and Normal-Weight Subjects." *Hepatology*, vol. 15, no. 5, 1992, pp. 795–798., doi:10.1002/hep.1840150508.

Umar, Umar Muhammad, et al. “Sonographic measurement of uterine dimensions in healthy nulliparous adults in Northwestern Nigeria.” *Sahel Medical Journal*, vol. 20, no. 1, pp. 1-7., doi:10.4103/1118-8561.204328.

U.S. Census Bureau. “Fertility of Women in the United States: 2018.” census.gov. 9 April 2019. Web. 3 April 2020. https://www2.census.gov/programs-surveys/demo/tables/fertility/2018/am-women-fertility/t3.xlsx

Wohlfahrt-Veje, Christine, et al. “Body Fat throughout Childhood in 2647 Healthy Danish Children: Agreement of BMI, Waist Circumference, Skinfolds with Dual X-Ray Absorptiometry.” *European Journal of Clinical Nutrition*, vol. 68, no. 6, 2014, pp. 664–670., doi:10.1038/ejcn.2013.282.

World Health Organization. “Obesity and Overweight.” World Health Organization, www.who.int/news-room/fact-sheets/detail/obesity-and-overweight. Accessed 27 March 2020.

Yifan Zhang

EDUCATION

Johns Hopkins Bloomberg School of Public Health Baltimore, MD
Master of Science (ScM), Biostatistics Expected May 2020

Johns Hopkins University Baltimore, MD
Bachelor of Science (B.S.), Biomedical Engineering May 2017
Combined B.S/M.S.E., Applied Mathematics and Statistics December 2017
Graduated with General Honors

BIOSTATISTICS EXPERIENCE

Intern February 2020-Present

Johns Hopkins Biostatistics Center

- Built logistic regression models in R to evaluate factors that affect post-mastectomy breast reconstruction utilization
- Produce Data and Safety Monitoring Board (DSMB) report using SAS

Graduate Research Assistant May 2016-Present

Johns Hopkins University, Department of Biostatistics/ Division of Biostatistics and Bioinformatics, Department of Oncology

- Downloaded, manipulated, and integrated sequencing and clinical data from The Cancer Genome Atlas (TCGA) database to be used in identifying mutational signatures associated with different environmental exposures in cancers of various types
- Performed mathematical extrapolations of organ sizes as a function of BMI based on literature search to investigate how obesity may lead to increased cancer risk

Intern November 2018-June 2019

Baltimore City Health Department

- Developed an indicators dashboard for the B'more for Healthy Babies initiative using R Shiny App
- Performed literature search to find case studies of how the use of R or other open source software was implemented at other organizations
- Designed and conducted a survey targeted at epidemiologists at the City Health Department to assess their R capacity and readiness
- Developed training material for lunch-and-learn R sessions

ADDITIONAL PROFESSIONAL EXPERIENCE

Undergraduate Research Assistant February-August 2017

Johns Hopkins University, Laboratory for Computational Sensing and Robotics

• Designed a study to evaluate the performance of the Robotic ENT Microsurgical System (REMS) in mastoidectomy procedures

• Assisted in designing a surgical phantom with CAD, and 3D printed the phantoms

• Developed a computer vision program in MATLAB for analysis of resulting phantoms from mock surgeries to quantitatively measure the effectiveness of the surgery

Undergraduate Research Assistant May-August 2015

University of Toronto, Departments of Molecular Genetics and Computer Science/ Mount Sinai Hospital, Lunenfeld-Tanenbaum Research Institute

• Selected to participate in the RTC Summer Research Program for Undergraduates

• Applied Barcode Fusion Genetics technology to assess the effects of DNA-damaging drugs on genetic interactions

Undergraduate Research Assistant May 2014-December 2015

Johns Hopkins University, Department of Biomedical Engineering/ University of Maryland School of Medicine, Department of Neurosurgery

• Developed a systematic method to generate reliable results with the CatWalk gait analysis tool, which was used to explore the viability of novel methodologies in promoting nerve regeneration after peripheral nerve injury

• Analyzed EEG recordings using MATLAB to assess the effects of therapeutic hypothermia on neurological recovery outcomes from cardiac arrest

High School Research Assistant June-August 2012

Yale School of Medicine, Neurology Department

• Explored the role of a number of intrinsic sequence motifs in targeting prestin to the lateral wall of outer hair cells (OHCs), a process critical for cochlear amplification

TEACHING EXPERIENCE

Teaching Assistant September 2019-Present

Statistical Methods in Public Health series (450 graduate students), Johns Hopkins Bloomberg School of Public Health, Department of Biostatistics

Teaching Assistant September-December 2016

Systems Bioengineering III (140 undergraduate and graduate students), Johns Hopkins University, Department of Biomedical Engineering

Tutor September 2014-December 2015

Johns Hopkins Learning Den

• Led small group tutoring sessions for a wide range of courses including Biology, Calculus, Differential Equations, Intro Programming in Java, Models & Simulations, Systems Bioengineering I

PUBLICATIONS

1. Diaz-Mejia J, Celaj A, Mellor J, Cote A, Balint A, Ho B, Bansal P, Shaeri F, Gebbia M, Weile J, Verby M, Karkhanina A, **Zhang Y**, Wong C, Rich J, Gupta G, Ozturk S, Durocher D, Brown G, Roth F. Mapping DNA damage-dependent genetic interactions in yeast via party mating and barcode fusion genetics. Molecular Systems Biology. 14 (5). 2018
2. Chen H, Du J, **Zhang Y**, Barnes K, Jia X. Establishing a reliable gait evaluation method for rodent studies. Journal of Neuroscience Methods. 283: 92–100. 201
3. **Zhang Y***, Moeini-Naghani I*, Bai JP*, Santos-Sacchi J, Navaratnam D. Tyrosine motifs are required for prestin basolateral membrane targeting. Biology Open. 4 (2): 197-205. 2015

CONFERENCE SUBMISSIONS

1. Du J, Xu C, **Zhang Y**, Jia X. The Effect of Cell Culture Passage on the Viability and Differentiation Capacity of Human Stem Cells in Rat Sciatic Nerve Regeneration. 39th Annual International Conference of the IEEE Engineering in Medicine and Biology Society; July 11-15, 2017; Jeju Island, Korea.
2. Du J, Chen H, **Zhang Y**, Jia X. Viability of Human Neural Crest Stem Cells across Cell-Culture Passages for Sciatic Nerve Regeneration. 8th International IEEE EMBS Conference on Neural Engineering; May 25-28, 2017; Shanghai, China.
3. Wang X, Chaudhry S, **Zhang Y**, Jia X. A Portable Wireless Multimodal Signal Acquisition System for Surface Electromyography Detection. 8th International IEEE EMBS Conference on Neural Engineering; May 25-28, 2017; Shanghai, China.
4. Navaratnam D, Moeini-Naghani I, Bai JP, **Zhang Y**, Santos-Sacchi J. Targeting of Prestin and Slo to the Basolateral Surface: Hair Cells Are Epithelial and Not Neuronal. Inner Ear Biology Workshop; November 1-4, 2014; Kyoto, Japan.
5. **Zhang Y**, Bai JP, Wu Y, Moeini-Naghani I, Santos-Sacchi J, Navaratnam D. Prestin is Trafficked to the Basolateral Surface of the Cell Using the AP1B Pathway. 37th Annual MidWinter Meeting of the Association for Research in Otolaryngology; February 21-26, 2014; San Diego, CA.
6. **Zhang Y**, Bai JP, Santos-Sacchi J, Navaratnam D. Prestin is Targeted to the Basolateral Membrane Using a Tyrosine Motif. 36th Annual MidWinter Meeting of the Association for Research in Otolaryngology; February 16-20, 2013; Baltimore, MD.

SKILLS

Technical: R, Python, MATLAB, SAS, Java
Languages: Chinese (Native), French (Elementary proficiency)